Science of the Total Environment 760 (2021) 143327

Contents lists available at ScienceDirect

Science of the Total Environment

journal homepage: www.elsevier.com/locate/scitotenv

Improving the spatial and temporal monitoring of cyanotoxins in Iowa lakes using a multiscale and multi-modal monitoring approach

Sarah B. Douglas Greene [a,b], Gregory H. LeFevre [a,b,*], Corey D. Markfort [a,b,**]

[a] Department of Civil & Environmental Engineering, University of Iowa, 4105 Seamans Center, Iowa City, IA 52242, United States
[b] IIHR-Hydroscience & Engineering, 100 C. Maxwell Stanley Hydraulics Laboratory, Iowa City, IA 52242, United States

HIGHLIGHTS

- Chlorophyll-a and microcystin concentrations were significantly related in Iowa lakes.
- The ELISA method conservatively estimates microcystin toxicity.
- Image mosaicing over water is possible using a geometry-based approach.
- Multispectral imaging predicted microcystin concentrations within 33%

GRAPHICAL ABSTRACT

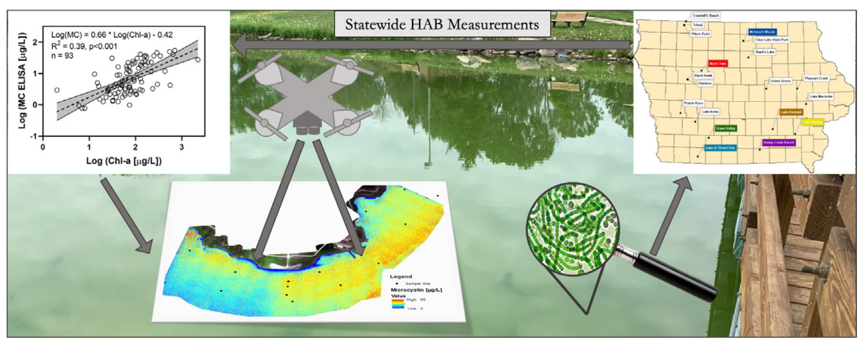

ARTICLE INFO

Article history:
Received 5 August 2020
Received in revised form 19 October 2020
Accepted 25 October 2020
Available online 13 November 2020

Editor: Kevin V. Thomas

Keywords:
Harmful algal blooms
Lake dynamics
Remote sensing
Unmanned aerial vehicle
Algal toxins
Microcystin congeners

ABSTRACT

Cyanobacterial harmful algal blooms (CyanoHABs) are pervasive and negatively impact lake water quality, resulting in economic losses and public health risks through exposure to cyanotoxins. Therefore, it is critical to better monitor and understand the complexity of CyanoHABs, but current methods do not fully describe the spatial and temporal variability of bloom events. In this work, we developed a framework for a multiscale and multi-modal monitoring approach for CyanoHABs combining drone-based near-range remote sensing with analytical measurements of microcystin cyanotoxins and chlorophyll-a. We analyzed weekly beach monitoring samples from 37 lakes geographically distributed across the state of Iowa (USA) over a 15-week period in the summer of 2019 to quantify ELISA (bioassay), 12 microcystin congeners (LC-MS/MS), and chlorophyll-a. We developed a novel microcystin congener-normalized equivalent toxin metric to compare CyanoHAB impacted waters; this microcystin-LR normalized sum-of-congeners approach yields lower predicted toxicity than parallel ELISA results suggesting ELISA is conservative for assessment. A significant linear relationship existed between chlorophyll-a and microcystin for lakes throughout Iowa ($R^2 = 0.39$, $p < 0.001$); lakes with low watershed: lake area ratio and long residence times exhibited a stronger correlation. We then developed a novel geometry-based image processing approach to allow for stitching over-water drone images, a previous barrier in photogrammetry. We applied our mutli-modal framework to a case study on Green Valley Lake to assess initial viability and predicted microcystin concentrations within 33%. We concluded that multispectral imaging is possible but may presently be insufficient for predicting microcystin concentrations due to limitations in the spectral capabilities of the multispectral camera, but technologies are quickly advancing, and lightweight hyperspectral imaging could soon become feasible for investigating spatial bloom variability on lakes.

* Correspondence to: G.H. LeFevre, 4105 Seamans Center, University of Iowa, Iowa City, IA 52242, United States.
** Correspondence to: C.D. Markfort, 323E Stanley Hydraulics Laboratory, University of Iowa, Iowa City, IA, United States.
E-mail addresses: gregory-lefevre@uiowa.edu (G.H. LeFevre), corey-markfort@uiowa.edu (C.D. Markfort).

https://doi.org/10.1016/j.scitotenv.2020.143327

1. Introduction

Cyanobacterial harmful algal blooms (CyanoHABs) occur in freshwater systems around the world, negatively impacting lake ecosystems by releasing cyanotoxins into the water, creating hypoxic conditions upon their decay, and impacting economies from decreased recreation (EPA, 2019). These blooms are created, in large part, from human influence of nutrient cycling through agricultural practices, leaving lakes of the Midwest United States particularly susceptible to bloom events (EPA, 2019). CyanoHABs are predicted to increase in frequency and severity due to climate change, with increased surface temperatures and changes in meteorological conditions promoting the growth and stability of blooms (Paerl et al., 2010, 2016). Therefore, it is important to understand the occurrence of bloom events, effectively monitor them, and prevent their negative impacts to the greatest extent possible.

Human exposure to cyanotoxins released from CyanoHABs occurs from contact with contaminated surface water and can result in pneumonia or respiratory distress, with mild impacts including fever, dermatologic, gastrointestinal, or other respiratory distress symptoms (Turner et al., 1990). Drinking contaminated waters can cause severe liver and kidney damage that result in livestock, pet, and human deaths (Da et al., 1993). The toxins present in a bloom are dependent on the cyanobacterial community because different species will release different toxins. Historically in the Midwest, microcystins have been the most common and dominant toxin present in blooms, found in 91% of 23 lakes sampled in a 2006 Midwest study (Graham et al., 2010). In Iowa specifically, microcystins were found in 100% of the 10 lakes sampled and was the dominant toxin in 90% of these samples. *Microcystis*, which only produce microcystin toxins, were detected in all Iowa lakes sampled in the 2006 study and in Green Valley Lake, Lake Keomah, and Lake of Three Fires in 2012 and 2013 samples analyzed by the State Hygienic Laboratory (State Hygienic Laboratory, Personal Communication, 2019). Therefore, although other toxins may be present in Iowa blooms, we focus on microcystins in this study due to their historical dominance. Microcystins are hepatotoxins, defined by an ADDA [(all-S,all-*E*)-3-amino-9-metoxy-2,6,8-trimethyl-10-phenyl-4(E),6(E)-dienoic acid] moiety common in the structure. Nevertheless, the two L-amino acids vary, generating over 300 structurally identified microcystin congeners as of 2020 (Bouaïcha et al., 2019; Jones et al., 2020), each with a different lipophilicity and polarity, resulting in a concomitant suite of toxicities. The known median lethal dose levels (LD_{50}) of microcystin congeners in mice ranges from 50 to greater than 1200 μg/kg (Chorus and Bartram, 1999). Not all congeners have been studied for their toxicological effects and not all congeners are quantifiable due to the lack of laboratory standards; indeed, only twelve congener standards were available for this study through Enzo Life Sciences (Enzo Life Sciences Inc., Retrieved from: https://www.enzolifesciences.com/product-listing/). Therefore, it is challenging to use congener profiles to predict bloom toxicity.

Several monitoring strategies have been developed for harmful algal blooms to assess toxicity quantitatively or qualitatively (Fig. 1). We will briefly review here five types of monitoring: bio-assay, chromatography, in-situ sensors and samplers, satellite remote sensing, and near-range remote sensing. ELISA (Enzyme-linked immunosorbent assay) test kits are a popular monitoring tool for assessing overall microcystin toxicity (EPA, 2012). However, the ELISA method cannot distinguish specific microcystin congeners, which has led to the development of liquid chromatography tandem mass spectrometry (LC-MS/MS) methods. LC-MS/MS methods can accurately quantify specific congeners with limited interference (EPA, 2012). Nevertheless, both bio-assay and chromatography methods are limited in their spatial and temporal resolution because they are collected from grab samples, requiring time, money, and personnel to collect. In-situ sensors are advantageous because they collect high temporal resolution data but rely on surrogate pigments such as chlorophyll-a or phycocyanin to quantitatively predict cyanobacterial abundance and infer toxicity. Also, these sensors are susceptible to fouling, requiring frequent maintenance and quality assurance for accurate readings (Davis et al., 1997). In-situ samplers, in contrast to sensors, collect automated water samples at set time intervals. These samples are preserved and later analyzed in the laboratory. Automated sampling allows for the quantitative assessment of cyanotoxins and their temporal trends (Miller et al., 2019), but still requires personnel, time, and money for sample analysis and

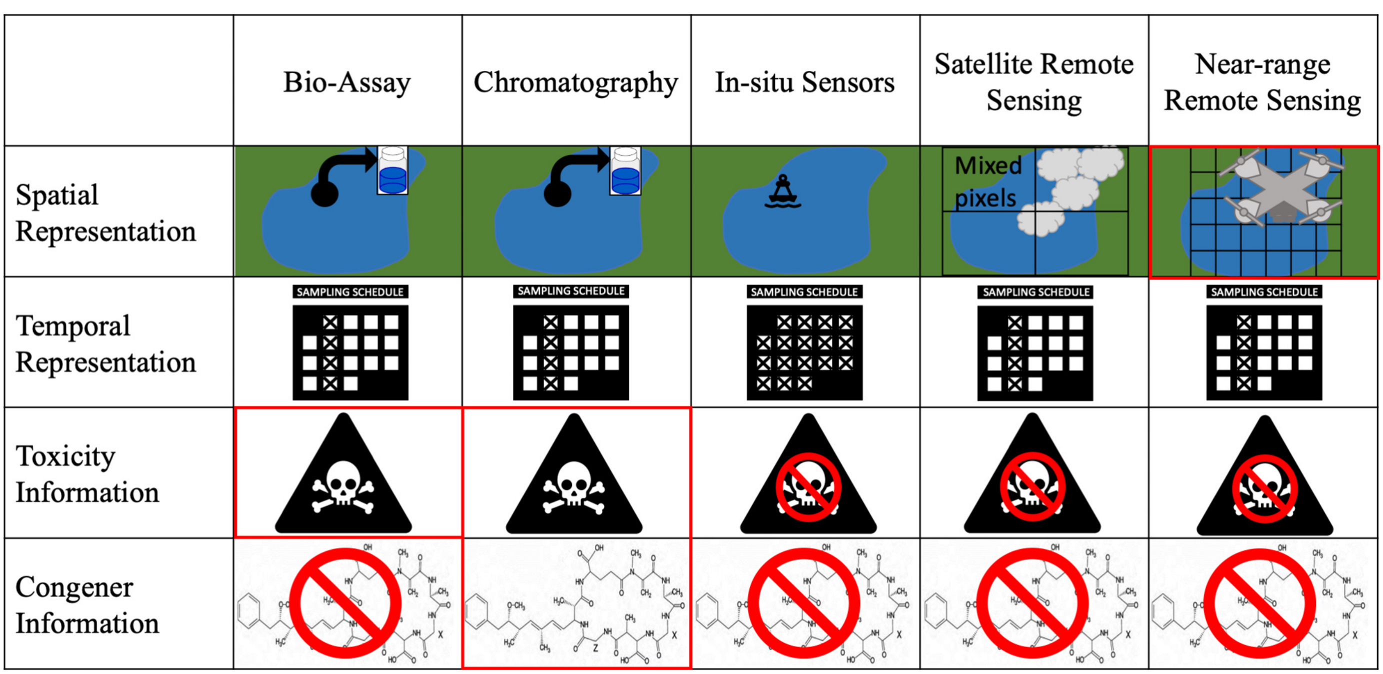

Fig. 1. Conceptual illustration of capabilities of HAB monitoring strategies. Red outlines indicate capabilities available when combining the specified analytical methods (i.e., bio-assay, chromatography) with near-range remote sensing, as proposed and conducted in this study.

maintenance. In-situ sensors and samplers are often placed on buoys, producing no spatial information. To improve spatial monitoring of blooms, remote sensing through satellites, small aircraft, and unmanned aerial vehicles (UAVs)/drones have become popular. Again, these strategies detect pigments and cannot directly measure toxicity. Satellite remote sensing has proven effective for ocean studies, large lake systems, or for assessing large-scale trends in blooms (Borbor-Cordova et al., 2019; NOAA, 2019). However, for small inland lakes, spatial resolution is too coarse to provide useful monitoring information, and cloud cover and mixed land/water pixels can prevent or complicate analysis (Kislik et al., 2018). Therefore, small aircraft and drone based near-range imaging technologies have emerged for monitoring of blooms on small inland lakes. The spatial resolution of near-range imaging can be sub-meter and there is greater flexibility in sampling time and location (Kislik et al., 2018). Because the spatial resolution is so high, several images are captured during monitoring, requiring image stitching. Over water image stitching has been a roadblock for these technologies due to the limitations of current photogrammetry software (Kislik et al., 2018).

There is no one monitoring strategy currently available to capture the spatial and temporal complexity of harmful algal blooms and predict toxicity. Therefore, we propose the use of a multiscale, multimethod approach using near-range imaging, bio-assay, and chromatography methods (indicated by the red lines in Fig. 1) to best capture bloom dynamics. The main limitation of remote sensing technologies is that they are unable to directly quantify the toxicity of blooms. However, a relationship has been identified that exists between the pigment chlorophyll-a and phycocyanin produced by cyanobacterial blooms and the toxins that they release (Francy et al., 2015; Hollister and Kreakie, 2016; Shi et al., 2015). We chose to use chlorophyll-a as the surrogate pigment in this study because it is readily detectable by more imagers, unlike phycocyanin which can only be detected by hyperspectral imagers and thus may be cost prohibitive to lake managers (Kislik et al., 2018). Additionally, phycocyanin methods have not been standardize and lack accuracy and reproducibility in the laboratory due to light and temperature sensitivity that cause rapid degradation (Kasinak et al., 2014). Understanding the relationship between chlorophyll-a and microcystin toxins and using it in conjunction with a remote sensing approach could allow for estimation of toxin levels using more practical, currently available technologies. An additional gap in the current monitoring of CyanoHABs in Iowa is the lack of data available on specific microcystin congeners and the implications of their concentrations on bloom toxicity. Therefore, the objective of this work was to determine microcystin congener abundance and toxicity in Iowa lakes, and then quantify the relationship between chlorophyll-a and microcystin toxins to predict the distribution of toxins using a near-range remote sensing approach. We developed, tested, and applied the drone-based monitoring technology framework for a case study lake and highlight the remaining hurdles to implementation as a novel lake monitoring approach.

2. Materials and methods

2.1. Weekly sampling procedures

The Iowa Department of Natural Resources (IDNR) conducts weekly microcystin sampling (on Tuesdays and Wednesdays) at Iowa's state-owned beaches from Memorial Day to Labor Day (US federal holidays; late May to early September). The IDNR uses a manual composite sampling technique centered in the swimming beach area (Fig. S.1). An additional 500 mL HDPE bottle was collected from a subset of the composite sample during normal state beach sampling by the IDNR to allow additional analyses for our study. The samples were transferred to a dark cooler with ice and transported, with temperatures not exceeding 10 °C, to the State Hygienic Laboratory's Coralville location, or to the Iowa Lakeside Laboratory (Milford, IA) location if collected in the northwestern portion of the state (Table S.1). The samples were then transferred to a fridge kept below 10 °C upon arrival to the appropriate laboratory. The samples sent to Lakeside Laboratory were filtered for chlorophyll-a analysis, with the filter frozen, and subsequently sent to Coralville for analysis by fluorometry. The remaining sample volume not used for chlorophyll-a filtration (only requiring a maximum of 100 mL, determined by sample turbidity as described in Section 2.1.2), was preserved and also sent to the Coralville location. Upon arrival, a 20 mL aliquot was transferred to a glass amber vial fitted with a PTFE screw cap and frozen for subsequent analysis of twelve microcystin congeners. Samples from locations other than Lakeside Laboratory were filtered for chlorophyll-a at the Coralville location, with a 20 mL aliquot reserved for congener analysis. The samples were transported in HDPE plastic (to permit safety and ease of handling during field collection and shipping) for a duration of one day to a week prior to transfer to glass, with longer transfer times for samples from Lakeside Laboratory.

In 2019, the monitoring season ran from May 21st to August 28th, with 37 beaches sampled across the state (Fig. S.2, Table S.1); however, not all 37 beaches were analyzed for chlorophyll-a and microcystin congeners weekly. Only samples that the IDNR reported with a microcystin concentration above 2 μg/L (above the drinking water advisory level of 1 μg/L (World Health Organization, 2004)) were further analyzed to lessen the sampling burden yet still capture significant bloom events. For each sampling period, 3 to 5 samples between 0.75 μg/L (ELISA limit of detection) and 2 μg/L were analyzed for the twelve congeners described below and compared to ELISA microcystin concentrations for quality assurance. In 2019, 20 beaches at 16 distinct lakes had observed ELISA microcystin concentrations greater than 2 μg/L (Fig. 2, top).

2.1.1. ELISA microcystin analysis conducted by IDNR

The IDNR analyzes for total microcystin using the microcystins/nodularins (ADDA) ELISA Kit, PN 520011 OH, Microtiter Plate (96T). IDNR follows the Ohio EPA Total microcystins – ADDA by ELISA analytical methodology (Zaffiro et al., 2016). The detection range is 0.15–5 μg/L, but the IDNR performs a 1:5 dilution on all samples, increasing the detection range to 0.75–20 μg/L. Additional dilutions are then conducted if the concentration exceeds 20 μg/L. A quality control standard, low calibration range check, and laboratory reagent blank are used for quality assurance. The samples are read in duplicate. ELISA beach monitoring results for 2019 and previous years can be found through the IDNR's water quality database, AQuIA (IDNR, n.d., Retrieved from: https://programs.iowadnr.gov/aquia/).

2.1.2. Chlorophyll-a analysis

The chlorophyll-a samples were analyzed by fluorometry using the State Hygienic Laboratory standard operating procedure, a modified version of EPA method 445.0 (Arar and Collins, 1997). First, a representative sample was collected on Millipore type SM, 47 mm 2.0 μm membrane filters by vacuum filtration in dim light to avoid photodegradation. Sample volume varied by the turbidity of the sample to prevent clogging of the filter, ranging from 10 to 100 mL, with volume recorded to determine correct chlorophyll-a concentration from the fluorescence measurement using the standard curve. Samples were ideally filtered within 24 h of collection, but sometimes up to 3 days following collection. The filter was stored and processed according to M445.0, except the samples were sonicated for 30 min rather than ground to release pigment (Arar and Collins, 1997).

The samples were analyzed using a Perkin Elmer Fluorometer, model LS using FL Winlab Version 4.00.02. Calibration standards were prepared using Sigma Chemical Chlorophyll-a standard stock diluted with aqueous 90% acetone. The exact concentrations of the calibration standards were determined using a spectrophotometer. The calibration curve was constructed using a blank and a minimum of 5 standards analyzed at room temperature, with the linear regression determined by the software. A minimum correlation coefficient

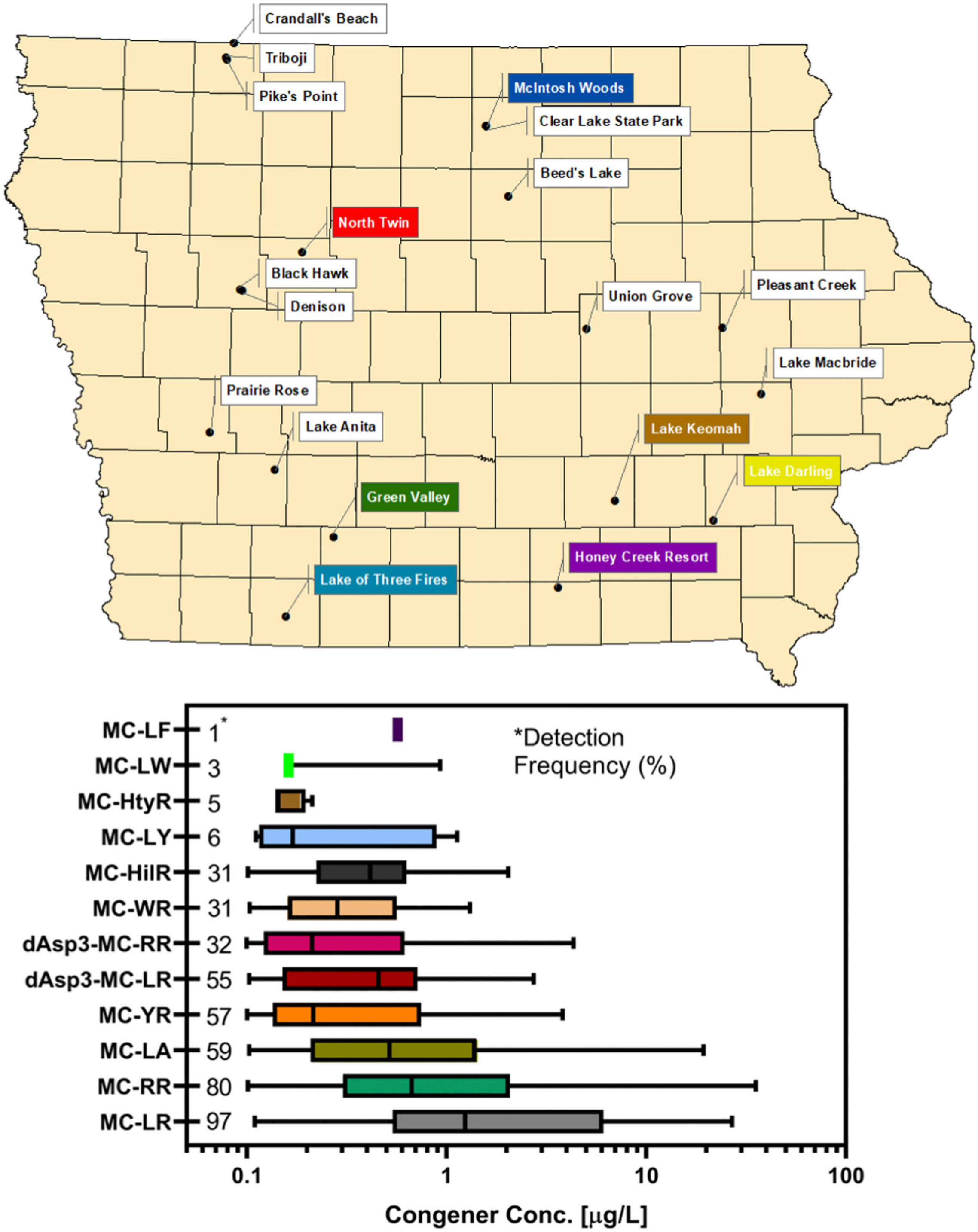

Fig. 2. State beach sites with microcystin levels above 2 μg/L by ELISA during the 2019 monitoring season. There were 20 distinct beaches at 16 lakes (top). Note: North Twin label includes the East and West beaches. The colored labels indicate vulnerable lakes, defined as lakes with 5 samples greater than 2 μg/L ELISA microcystin. Concentration distributions of 12 microcystin congeners and their detection frequencies in the 87 analyzed samples with ELISA microcystin concentrations above 2 μg/L in 2019 Iowa state beach samples (bottom). Boxplots represent median, interquartile range, and min/max values. Note: The color schemes for the vulnerable lakes and microcystin congeners in this figure are consistent with later figures.

of 0.999 was required for the standard curve. A sipper cell system was used to pull samples. Lab reagent blanks, control blanks, quality control standards, and lab duplicates were added throughout each run to ensure all quality control and assurance requirements were met. If dilutions were required, they were conducted using 90% acetone. The sample intensities were converted to concentrations by the software based on the linear regression curve and corrected for filtered volume.

2.1.3. Microcystin congener analysis

As described in 2.1, the samples were transferred to 20 mL glass amber vials and frozen at −20 °C until analysis. Three freeze-thaw cycles were conducted to lyse the cyanobacterial cells, agitating the samples after each cycle. Then, the samples were filtered through a 25 mm, 1.2 μm glass-fiber filter. 0.5 mL of sample were added to sample vials, with 25 μg/L of 100 ng/mL Simeton added to each sample as internal standard. The prepared samples were stored at −10 °C until analysis.

The target analytes included twelve microcystin congeners: MC-LR, MC-RR, MC-LA, MC-YR, MC-LY, MC-LF, MC-LW, MC-WR, [dAsp^3] MC-LR, [dAsp^3] MC-RR, MC-HtyR, and MC-HilR (Table S.2). The standard calibration curve was prepared using stock standards of the twelve congeners and diluted using 10% methanol in water, with Simeton added as internal standard. Calibration range was 0.1–10 μg/L.

The samples were analyzed via HPLC-MS/MS using a Dionex Ultimate 3000 UPLC and Velos Pro linear ion trap mass spectrometer. The HPLC Column used was an Agilent Zorbax SB-C18 RRHD, 2.1 × 150 mm, 1.8 μm. Mobile phase A was 0.1% formic acid in water and mobile phase B was 0.1% formic acid in acetonitrile. Flow rate of mobile phase was 0.3 mL/min with ramp increase in mobile phase B from 10% to 90%. From 2 min to 16 min, mobile phase B increased from 10 to 80%. At 16.1 min, mobile phase B increased to 90% and was held until 22 min. At 22.1 min, mobile phase B was decreased back to 10%. The mass spectrometry details can be found in Table S.3. XCalibur software was used for quantification. Samples above 10 μg/L were diluted and re-analyzed. A 10% methanol solution was used as the lab reagent blank. Standards were used periodically during runs to ensure consistent retention times and peak areas.

2.1.4. Regression analysis and statistics

Chlorophyll-a and microcystin data were tested for normality using the Kolmogrov-Smirnov test and were not statistically significantly different from a log-normal distribution at the 90% confidence level. Therefore, a log-log linear regression was applied as a best-approximation for data distribution when determining the relationship between chlorophyll-a and microcystin. F-Tests on the slopes and intercepts of the linear regressions were performed in Minitab and reported with *p*-values tested at the 95% confidence interval. The coefficient of determination (R^2) was used as a metric for goodness of fit and 95% confidence intervals about the regression line were calculated in GraphPad Prism (version 8). A Pearson's correlation analysis was conducted in GraphPad Prism to relate the coefficient of determination for lake-specific regressions to other lake parameters: watershed:lake area ratio, mean depth, residence time, and internal phosphorus loading. A one-way matched pair ANOVA followed by a Tukey's multiple comparison analysis was used to compare toxicity metrics including ELISA, Congeners, and $MC\text{-}LR_{\text{Toxic equivalents}}$ (as detailed in Section 3.2).

2.2. Case study methods

A study was conducted on Green Valley Lake on August 15th, 2019 to determine the potential of a multispectral/UAV remote sensing approach for predicting and mapping the distribution of microcystin toxins in Iowa lakes. Green Valley Lake was chosen as an ideal case study site due to the prevalence of pervasive blooms on the lake over the last several years. The lake is located in Union County (S26, T73N, R31W), about 2.5 mi NW of Creston, Iowa in a 5175-acre watershed (Fig. S.3). The lake area is 386 acres with a mean depth of 10.5 ft. A flight area centered on the swimming beach was chosen due to accessibility, data availability throughout the summer at the beach through the state beach monitoring program, and location of sensors with additional water quality data through Iowa State University (Fig. S.4). Grab samples were collected throughout the flight area, with samples collected at the two sensor stations and a transect of densely collected samples toward the beach area to capture the extent of horizontal heterogeneity. These samples were analyzed for chlorophyll-a, total microcystin, and microcystin congeners using the methods described above. The beach is just north of sample site 7, and a boat launch access is located just north of sample site 11.

2.2.1. Sample collection

A boat was used to traverse the lake and a handheld GPS system was used to navigate to the sampling sites. The location coordinates were recorded for each sampling site (Fig. S.5). 250 mL PETG bottles were used to collect the samples, after rinsing with source water three times just deep enough to submerge the bottle. The samples were then immediately placed on ice in an opaque cooler to protect the samples from light degradation and heat. As a quality control measure, a duplicate sample was collected at sensor 5 and sample site 14. Dissolved Oxygen, temperature, pH, and conductivity were collected at each site using a Hach HQ40D portable water quality sonde. The samples were analyzed and filtered for chlorophyll-a at the State Hygienic Laboratory the following day.

2.2.2. Flight planning

A MicaSense Rededge-3 (Micasense Inc., WA, USA) multispectral camera mounted on a DJI Inspire 1 drone (DJI, China) was used to collect image data over the flight area of 148,178 m^2. Due to battery limitations, three flights were required to cover the total study area. The drone operated at a height of 90 m above the surface, and at a flight speed of 6 m/s, to obtain a 75% image overlap (Fig. S.5). The MicaSense Atlas Flight application was used for flight planning and the DJI GO application was used to control the drone during flight. The weather conditions at the beginning of the flight were cloudy with intensifying light rain and wind as the flight proceeded. Over 400 multispectral images were obtained, with 5 bands for each image.

2.2.3. Image processing workflow

The raw images collected from the Micasense camera were first georeferenced and rotated using metadata collected by the drone and camera systems and raw images were converted to reflectance. The images were then mosaiced and band math algorithms were applied. The geo-referencing, rotating, and conversion of the images to reflectance was conducted using a Python script. The images were mosaiced and band math algorithms were applied using Erdas Imagine software (Hexagon AB, Sweden).

First, the images were georeferenced by writing world files for each image to describe the location, scale, and extent of rotation for each image to be read by Erdas Imagine software. A world file is a short text file associated with an image with the following terms: dimension of pixels in x-direction, rotation in x-direction, rotation in y-direction, dimension of pixels in y-direction, x-coordinate of the upper left pixel, and y-coordinate of the upper left pixel. The coordinates of the upper left pixel were calculated from the directional vector transformed from a rotational matrix based on the orientation of the camera at the time of image capture (Fig. S.8). The pixel dimensions and rotations were calculated from the camera specifications and flight altitude and transformed with appropriate trigonometric functions (Eqs. (S.1)-(S.7)). See SI for Python script. The same process was applied to all images.

After generating the world files for each image, the raw image values were converted to reflectance (Eqs. (S.8), (S.9)). Micasense released a Python package on GitHub to convert images to reflectance, the functions of which were adapted and used in the analysis (Micasense Inc., 2017). The python script used to convert band 1 is provided in the SI, as an example, with similar analysis performed for the other 4 bands. The analysis sequence was to first use calibration images to convert each image from radiance to reflectance, followed by correction for vignetting and lens distortion, and then to save the undistorted reflectance image as a new file. The reflectance images were brought into Erdas with their associated world files to mosaic the images into one scene. Quality control was conducted manually to remove images that did not stitch together properly. Each band was mosaiced using the same parameters (see SI for details). The five mosaiced bands were then layer stacked to combine them into a single image and then band math algorithms were applied.

Several multispectral band math algorithms have been developed, many for satellite applications and some have been investigated for monitoring HABs. The Micasense RedEdge-3 has five bands, including red, green, and blue, as well as Red Edge and near infrared (NIR) bands outside of the visible spectrum (Table S.4). Not all algorithms that have been developed are applicable for use with the Micasense RedEdge. For example, some Landsat-8 algorithms use the coastal blue band, which is not measured by the RedEdge. The following algorithms were applied in the analysis: BNDVI, SABI, NDVI, FLH Blue, Kab1, NDRE, KIVU, and SHI (Table S.5).

3. Results and discussion

3.1. Prevalence and spatiotemporal variability of microcystin congeners

Microcystin congener distributions have not been extensively studied in the Midwest or Iowa (Graham et al., 2010); consequently, there is a lack of understanding of microcystin congeners that may be present in a bloom or if any spatial or temporal trends exist. Therefore, we first identified the prevalence of 12 microcystin congeners in Iowa lakes. MC-LR and -RR were the most abundant of the 12 congeners we quantified in the beach monitoring samples, present in 97% and 80% of the 87 samples analyzed, respectively (Fig. 2, bottom). MC-LR and -RR abundance is consistent with previous findings in the Midwest and other locations in the United States, and Asia (Díez-quijada et al., 2019; Graham et al., 2010). The mean and maximum concentrations were also greatest for the most prevalent congeners (Fig. 2, bottom). We tested for two alternative algal toxins, cylindrospermopsin and anatoxin-a in 25 of the samples using EPA method 545 (U.S. EPA, 2015). No concentrations of cylindrospermopsin and anatoxin-a were above the detection levels (0.04 and 0.0133 μg/L, respectively) in any sample, consistent with previously reported studies in the Midwest that suggest microcystin toxins dominate (EPA, 2016; Graham et al., 2010).

To investigate the spatial and temporal variability of microcystin congeners in Iowa, we generated time-series data for the five most common congeners of the twelve quantified (MC-LR, -RR, -LA, -YR, and [dAsp3] MC-LR) at seven Iowa lakes (Fig. 3, Fig. S.9). These lakes had five or more samples with ELISA microcystin concentrations ≥2 μg/L and will herein be defined as "vulnerable lakes". No clear spatial or temporal trends emerged in the distribution of congeners or their concentrations in the vulnerable lakes. McIntosh Woods had a constant low concentration of microcystin with no clear peak in any individual congener, whereas the other vulnerable lakes had a spike near the middle or end of the season. Green Valley Lake and Lake of Three Fires are both located in the southwestern portion of Iowa, but exhibited markedly different congener distributions. Lake of Three Fires was MC-LR dominant and Green Valley Lake was MC-RR dominant for the majority of the season. Similarly, Lake Darling, Lake Keomah, and Honey Creek Resort are close geographically (within 100 km), but had distinct congener profiles. Higher temporal resolution data may be needed, but these initial results in Iowa indicate that blooms are rapidly changing systems that are often unpredictable. Previous research in the Great Lakes and Ontario region also reported variability in MC-LA, MC-LR, MC-RR, and MC-YR distributions from lake to lake, with potential distribution patterns caused by environmental factors rather than geographic location (Taranu et al., 2019). Our study did not capture nutrient concentrations or meteorological conditions necessary to compare

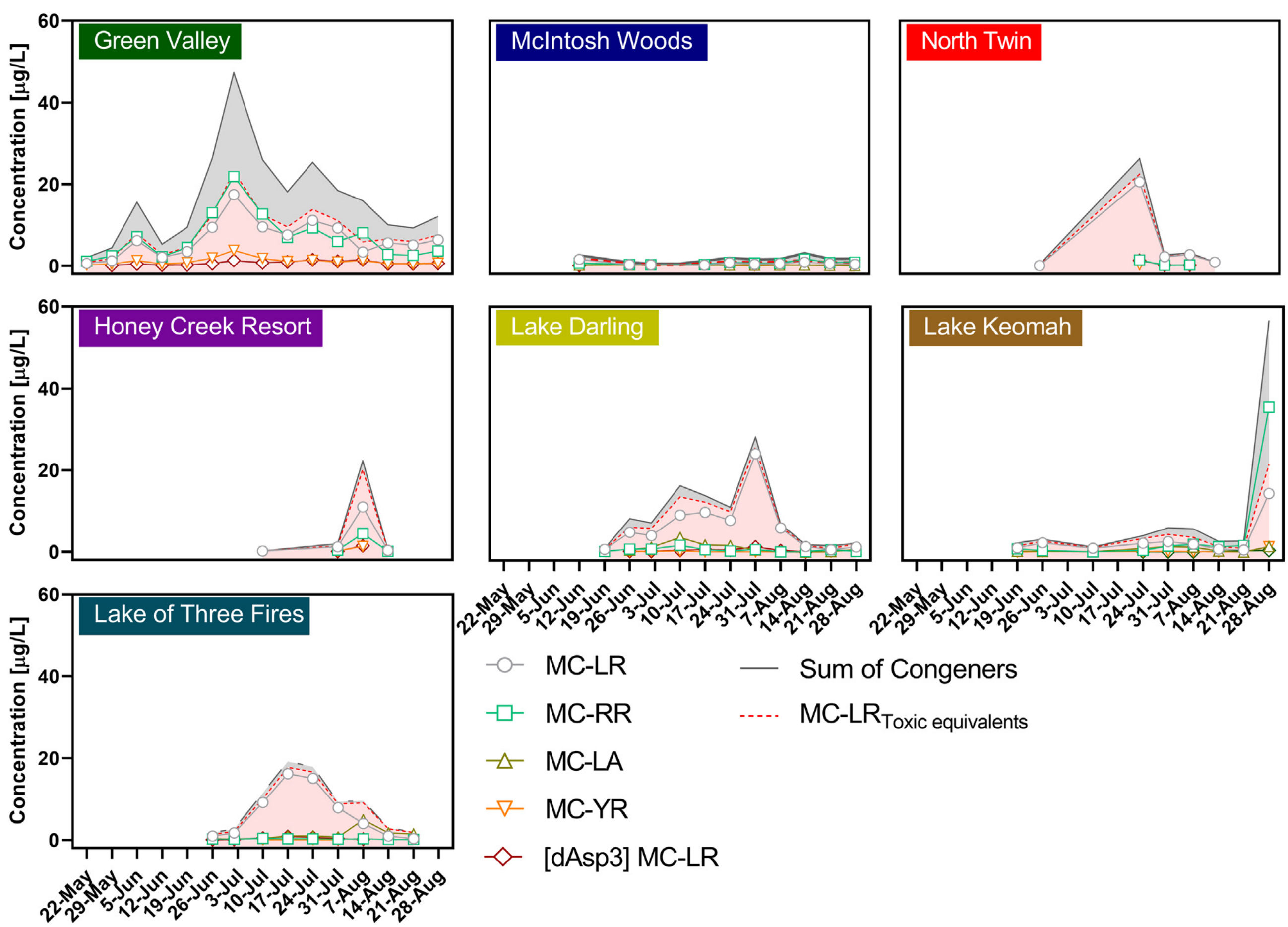

Fig. 3. Distribution of the top five most common congeners (of the twelve quantified) in the 2019 beach samples at the seven "vulnerable lakes" (≥5 samples ≥2 μg/L ELISA microcystin). Sum of congener concentrations and MC-LR$_{\text{Toxic equivalents}}$ concentrations shown with grey and red below area shading, respectively. Axis scales are the same in all panels to allow efficient visual comparison of concentration trend values between lakes. A log-axis version of these results is in Fig. S.10 as alternative to highlight the concentration differences visually.

with their findings, but capturing these data in future studies could be useful for helping to predict congener abundance. Additionally, characterizing the cyanobacterial community could be beneficial in predicting the presence of certain microcystin congeners. Although *Microcystis* are the most common microcystin producers, *Anabaena*, *Planktothrix*, *Oscillatoria*, and other species can produce not all, but some congeners (H. K. Hudnell, 2008). Therefore, classifying the bacterial community could aid in predicting which congeners are most likely to be present in a sample. However, this information alone will not allow for prediction of the concentration of those congeners.

3.2. A novel microcystin congener normalized toxicity framework

Our analysis of congener data suggests that the ELISA method may not reflect the true toxicity of microcystin-dominant cyanobacterial blooms given the variability of congeners present, each with differing toxicities and abundance, in the lake water samples. We conceptualized a new normalized toxicity metric to determine if the congener-independent method (ELISA) is effective for predicting toxicity, rather than overall microcystin concentration. The ELISA method is often used for assessing public health risk, thus evaluating its efficacy in the context of multiple microcystin congeners is critical. MC-LR has been studied extensively for toxicity because it is the most common and abundant congener across many freshwater lake systems (Díez-quijada et al., 2019; Graham et al., 2010); thus, MC-LR has been used as a toxicity predictor to set advisory levels (Testai et al., 2016; World Health Organization, 1998). Because each congener exhibits different toxicity, we normalized all congener concentrations measured to MC-LR$_{\text{Toxic equivalents}}$ using Eq. (3.1) based on literature-reported LD_{50} values in mice (Table S.7). It should be noted that this proposed novel framework for normalizing MC-LR$_{\text{Toxic equivalents}}$ is distinct from prior concepts of congener normalization, which are based not on toxicity but rather on relative analytical quantification (Natumi and Janssen, 2020).

$$\mathrm{MC-LR}_{\textit{Toxic equivalents}} = \mathrm{MC-XX}_{\textit{Measured}} \times \mathrm{MC-XX}_{\textit{Equivalent factor}} \quad (3.1)$$

where,

$$\mathrm{MC-XX}_{\textit{Equivalent factor}} = \frac{\mathrm{LD}_{50}(\mathrm{MC-XX})}{\mathrm{LD}_{50}(\mathrm{MC-LR})},$$

$\mathrm{MC}-XX_{\textit{Measured}}$ = measured microcystin congener concentration

We compared the 2019 beach sampling results from across Iowa between using the ELISA, sum of congeners (sum of 12 individual congener concentrations), and MC-LR$_{\text{Toxic equivalents}}$ concentrations methods (Fig. 4). To determine if congener dominance in the lake impacts method performance, we also binned the samples into three groups by dominant congener: MC-LR, MC-RR, and MC-LA. Twenty-one of the 93 samples analyzed were above the advisory level of 20 μg/L by ELISA; however, only 7 samples were >20 μg/L MC-LR$_{\text{Toxic equivalents}}$ (Fig. 4a). The ELISA method concentration was significantly greater than the MC-LR$_{\text{Toxic equivalents}}$ ($p < 0.001$) for all groups, indicating that the ELISA method could be overestimating the toxicity of blooms. This is particularly noticeable when MC-RR is the dominant congener in the sample due to its low relative toxicity (Fig. 4c). This trend is also notable when examining the Sum of Congeners and MC-LR$_{\text{Toxic equivalents}}$ time series data for Green Valley Lake (MC-RR dominant) and Lake of Three Fires (MC-LR dominant) (Fig. 3). MC-LF and MC-LW are the most toxic congeners (Faassen and Lurling, 2013), but were the least prevalent in our samples (Fig. 2). These congeners were only present when ELISA microcystin concentrations were >20 μg/L and surface water temperatures were >25 °C, conditions where cyanobacteria growth is maximum (K. Hudnell, 2008). With a changing climate, elevated temperatures could become more prevalent, resulting in greater concentrations of the highly toxic congeners and subsequent potential for underestimation of bloom toxicity using congener independent approaches (i.e., ELISA microcystin).

Alternatively, the sum of congener and MC-LR$_{\text{Toxic equivalents}}$ could underestimate concentrations in comparison to ELISA. The samples were stored in HDPE plastic temporarily, which could have resulted in adsorptive losses (Altaner et al., 2017; Zaffiro et al., 2016). Adsorptive

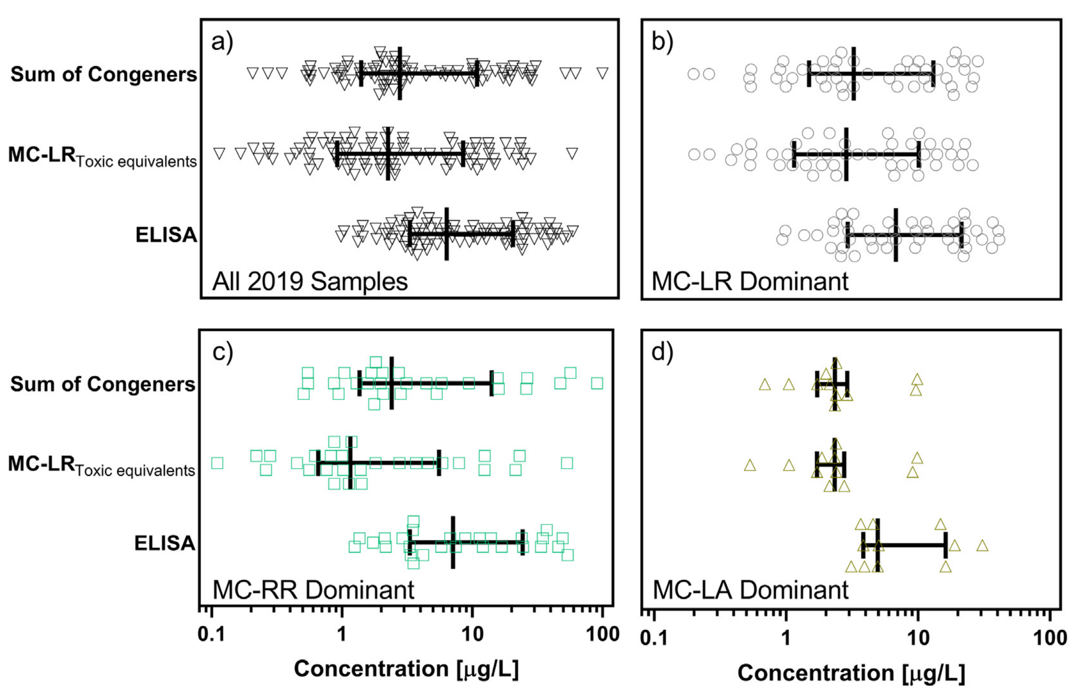

Fig. 4. Comparison of the of ELISA method to toxicity-normalized MC-LR$_{\text{Toxic equivalents}}$ determined from LC-MS/MS method. The ELISA method concentration was significantly greater than the MC-LR$_{\text{Toxic equivalents}}$ ($p < 0.001$). Comparison of ELISA, MC-LR$_{\text{Toxic equivalents}}$, and Sum of Congener concentrations for the (a) 2019 beach samples. The second-fourth panel show samples where (b) MC-LR, (c) MC-RR, and (d) MC-LA were the dominant congener in the sample, respectively. Bars indicated medians and interquartile range.

losses would decrease observed congener concentration by the LC-MS/MS method as compared to the ELISA because ELISA samples were collected in non-adsorptive PETG plastic. Only 12 of the potential congeners were quantified due to a lack of access to analytical standards for other congeners, whereas ELISA generates a response for all possible microcystin congeners and nodularin. We suggest as a framework going forward first to screen and identify the congeners of greatest abundance and toxicological relevance, and then prioritize availability of those analytical standards for improved monitoring. From reported toxicity information (as LD_{50} values in mice), some congeners that should be prioritized are: MC-YA (60–70 μg/kg), [D-Asp^3,(E)-Dhb^7]MC-LR (70 μg/kg), [ADMAdda^5]MC-LR (60 μg/kg), MC-YM(O) (56 μg/kg), [ADMAdda^5]MC-LHar, and [D-Asp^3,(E)-Dhb^7]MC-HtyR (70 μg/kg) (Bouaïcha et al., 2019). As standards become available for more congeners, this relative toxicity framework should be further developed with efforts to minimize adsorptive losses to the greatest extent possible. Then, a more complete assessment of the ELISA method as a toxicity tool can be conducted.

Recently, additional efforts have been made to analyze more or potentially all microcystins by LC-MS. Munoz et al. (2017) presented use of Lemieux-von Rudloff oxidation to produce the 2-methyl-3-methoxy-4-phenylbutyric acid (MMPB) moiety from each microcystin, which can then be analyzed as one integrated compound representing nearly all MCs and nodularins. The advantage to using an approach that oxidizes microcystins to a common moiety for analysis is that measurements via LC-MS are not limited to only the targeted congeners (i.e., $n = 12$ in our work); however, the disadvantage is that resolution is lost on what congeners were present and does not factor in differential toxicity of the various congeners. Indeed, the oxidation to a common moiety approach is useful for comparison to ELISA data, but was not explored in this study. Natumi and Janssen (2020) used a suspect screening approach and a (sub)class specific quantification based on most-similar laboratory standards available, a technique that is more accurate than only MC-LR-equivalents concentrations (notably, based on chemical analysis not toxicity, as described above). The application of non-target and suspect screening high-resolution mass spectrometry for algal toxins will enable enhanced understanding of microcystin congener profiles in lakes as this technology gains wider-spread use. Growing advances in mass spectrometry technology and techniques will improve measurements of microcystin in aquatic systems.

3.3. Predicting microcystin concentrations from chlorophyll-a in Iowa Lakes

We discovered a statistically significant linear relationship between log chlorophyll-a and log ELISA microcystin concentrations in samples from the lakes across Iowa ($R^2 = 0.39$, $p < 0.001$; Fig. 5a). Our results suggest that a state-wide relationship may be able to predict microcystin concentrations from chlorophyll-a in Iowa lakes. A similar relationship occurred between chlorophyll-a and the sum of congeners ($\text{Log (MC)} = 0.87 * \text{Log (Chl-a)} - 1.11$, $R^2 = 0.46$, $p < 0.001$; Fig. S.11). The microcystin ELISA samples span 20 different beach sites at 16 lakes, covering all geographic regions of the state and over a 99-day spread of

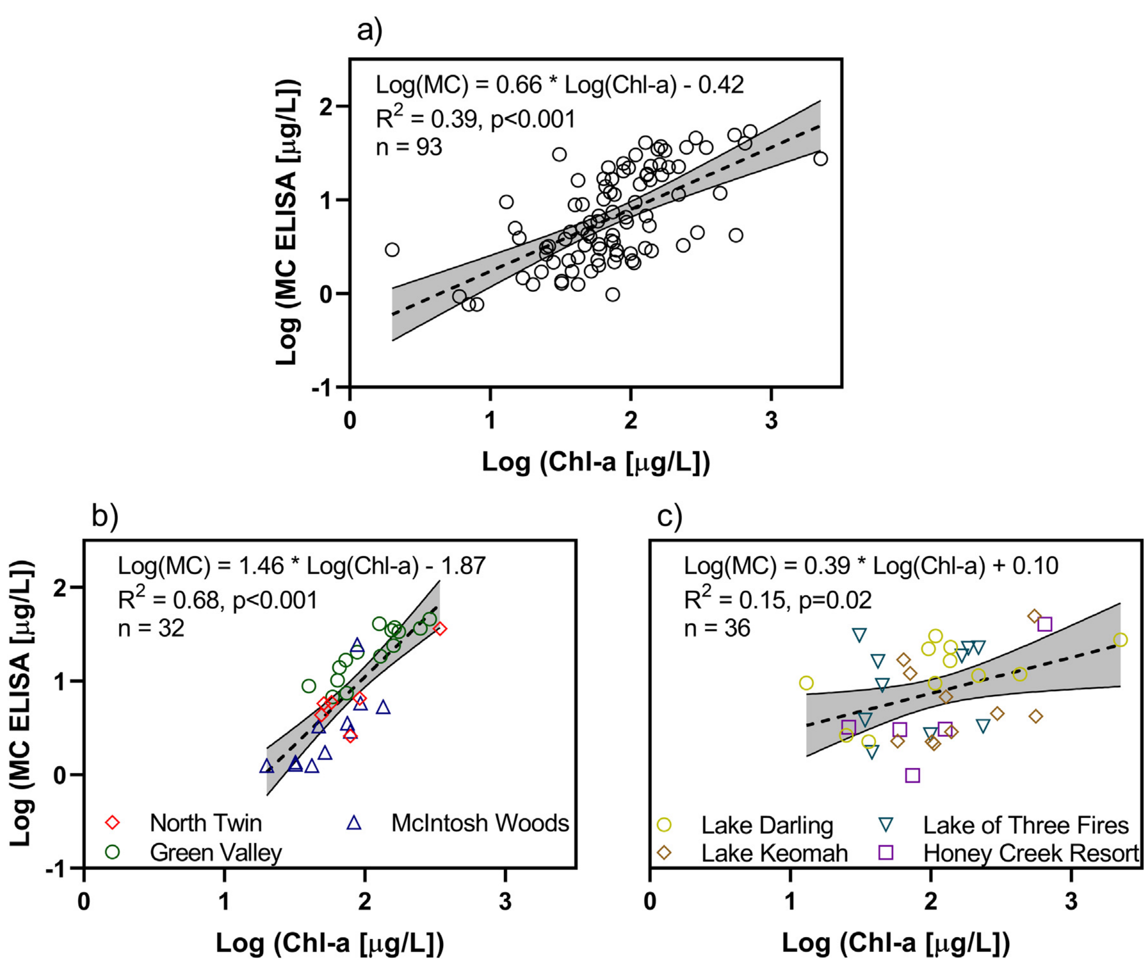

Fig. 5. Quantifying the chlorophyll-a/microcystin relationship in 2019 beach samples. (a) Log-log linear relationship between chlorophyll-a and ELISA microcystin for all 2019 samples. The microcystin ELISA samples spanned 20 different beach sites at 16 lakes, covering all geographic regions of Iowa over a 99-day sampling period. Relationship for vulnerable lakes (≥5 samples exceeding 2 μg/L ELISA microcystin) with (b) strong relationships; coefficients of determination greater than 0.5 and statistically significant slopes and (c) weak relationships. Shaded regions indicate 95% confidence intervals about the regression line.

sampling (Fig. 2). Despite the natural variability inherent to environmental samples and the diversity of the samples in geographic location, lake characteristics, and time, the relationships were still significant. A positive relationship between chlorophyll-a and microcystin health advisories is consistent with observations for lakes across the contiguous United States (Hollister and Kreakie, 2016), suggesting broader utility in estimating microcystin from pigments. This study was only conducted for one season, thus the long-term stability of the chlorophyll-a/microcystin relationship should be confirmed in future work. A study at Lake Taihu, China reported multi-year temporal stability of a chlorophyll-a/microcystin relationship (Shi et al., 2015); therefore, it is possible that individual lakes maintain stability of this relationship over multiple seasons.

3.3.1. The chlorophyll-a/microcystin relationship is variable for vulnerable Iowa Lakes

We developed specific relationships between chlorophyll-a and microcystin for each of the seven vulnerable lakes (Table S.8) to examine if there were differences in relationship strength between waterbodies. The vulnerable lakes with coefficients of determination greater than 0.5 and statistically significant slopes were defined as "strong relationship" lakes and all others were defined as "weak relationship" lakes. The strong relationship data were pooled, and an overall regression was generated (Fig. 5b) with lakes including Green Valley, North Twin, and McIntosh Woods Lake. Weak relationship lakes included Lake Keomah, Lake of Three Fires, Lake Darling, and Honey Creek Resort Lake (Fig. 5c). Green Valley Lake exhibited the strongest relationship, with chlorophyll-a predicting 78% of the microcystin variability. Lake of Three Fires had the weakest relationship, with chlorophyll-a only explaining 3% of the microcystin variability. Our results suggest that the relationship between chlorophyll-a and microcystin varies significantly between Iowa lakes, but it is not clear why. Therefore, we investigated if specific lake factors may drive the relationship variability.

3.3.2. Watershed:lake area ratio and residence time impact the chlorophyll-a/microcystin relationship

To probe underlying drivers causing variability in the chlorophyll-a/microcystin relationships across lakes, we investigated the following lake characteristics: residence times, watershed:lake areas, internal phosphorus loadings, and mean lake depths obtained from previously published data (Tables S.9 and S.10). For each characteristic, we conducted a Pearson's correlation analysis with the corresponding coefficient of determination from the vulnerable lakes (Fig. S.12). Watershed:lake area ratio was negatively correlated with the coefficients of determination from the seven vulnerable lakes ($r = -0.66$, $p = 0.11$). A smaller watershed:lake area ratio may be favorable for the use of a simple linear relationship to predict microcystin, whereas a larger ratio may not be well characterized by a univariable model. As watershed:lake area ratio increases, lakes become more difficult to manage and less predictable due to complex nutrient loading dynamics of larger watershed systems and less in-lake assimilation capacity (Ikenberry, 2012). Residence time was positively correlated ($r = 0.43$, $p = 0.33$), indicating that longer residence times may be favorable for the use of a simple linear model to predict microcystin concentrations from chlorophyll-a. Longer lake residence times result in more favorable conditions for stable bloom development (K. Hudnell, 2008). We recognize that these correlations presented are not at a 95% significance level, likely due to the small sample size; however, the results are consistent with the cited literature. Mean lake depth ($r = -0.10$, $p = 0.83$) and internal phosphorus loading ($r = 0.36$, $p = 0.43$) had weak correlations with the coefficient of determination that were not significant and, consequently, were not explored further.

We also plotted the cumulative coefficient of determination against increasing watershed:lake area ratio and decreasing residence time for all lakes (Fig. 6a and b) to examine if a break-point exists in the strength of prediction. A decrease in the coefficient of determination occurred above watershed:lake area ratios of 20 and below residence times of 47 days (Fig. 6a and b; red lines). Limiting analysis to lakes with watershed:lake area ratios ≤20 or residence times ≥47 days, yielded a stronger relationship ($R^2 = 0.55$ and 0.50, respectively; Fig. 6c and d) than when including all lakes (Fig. 5a). When the watershed:lake area ratio or residence times are known for a lake and meet the defined criteria, the refined regressions could be applied for increased accuracy in predicting microcystin concentrations. Understanding the impact of commonly measured physical/chemical lake characteristics broadens the impacts of our discoveries; future investigations outside Iowa can compare to our findings herein.

3.4. Green Valley case study: developing new HAB remote sensing approaches

We chose Green Valley Lake as an ideal case study for testing the utility of drone-imagery remote sensing technologies, based on historical occurrence of HAB events and our data demonstrating a significant chlorophyll-a/microcystin relationship. We collected sixteen samples within the proposed flight area to validate the predictions of chlorophyll-a (Fig. 7, top). Sample sites 7 and 9, the sites closest to the swimming beach, had the highest measured chlorophyll-a, ELISA microcystin, and congener concentrations in the study area. These sites were in the shallowest regions closest to the shore, where algal scums are more likely to form (K. Hudnell, 2008). Although the total concentrations were highest in these locations, the relative proportions of the congeners remained comparatively consistent. Thus, the profiles of congeners on a single lake may be spatially consistent, although not between different lakes, as we observed in the results from across the state. This hypothesis would require further testing across different lakes and at multiple time points. The concentrations of chlorophyll-a and microcystin were substantially higher for site 7 (closest to the beach site) than the concentrations found from the composite beach sample collected by the IDNR on the previous day. These findings indicate that even on a one-day time scale, we observed significant variability in concentration, further supporting our findings that HAB systems are highly variable in space and time.

3.4.1. Chlorophyll-a/microcystin relationship for Green Valley Lake was spatially and temporally consistent

The predictions for microcystin from chlorophyll-a, using the same regression approach described above, were not significantly different between the case study (Fig. 7, bottom) and the state beach monitoring data ($p = 0.96$) collected throughout the summer season at Green Valley Lake. Therefore, the relationship between chlorophyll-a and microcystin on Green Valley Lake was temporally and spatially consistent in 2019, but longer-term stability should be verified. For other lakes in Iowa, it is unknown if spatial consistency of the chlorophyll-a and microcystin relationships exists, which should be a focus of future research. Studies on Lake Taihu, a hypereutrophic lake in China significantly impacted by CyanoHABs, report positive and consistent chlorophyll-a/microcystin relationships across multiple years and from various sampling locations (Shi et al., 2015). It is possible then, that Green Valley Lake, also hypereutrophic, may exhibit multiannual consistency. This discovery is valuable because multiannual and spatial consistency in the correlation at lakes makes models developed in prior years useful for making future measurements without the need for further sampling and model adjustment. At lakes where multiannual consistency is not observed, chlorophyll-a and microcystin relationships would need to be updated annually to facilitate remote sensing predictions of microcystin concentrations.

3.4.2. A geometry-based image processing approach for near-range remote sensing of HABs

We applied the image processing workflow (described in Section 2.2.3) to the multispectral imagery collected during the Green Valley case study and tested eight previously developed band math algorithms for their ability to predict chlorophyll-a. The SHI index

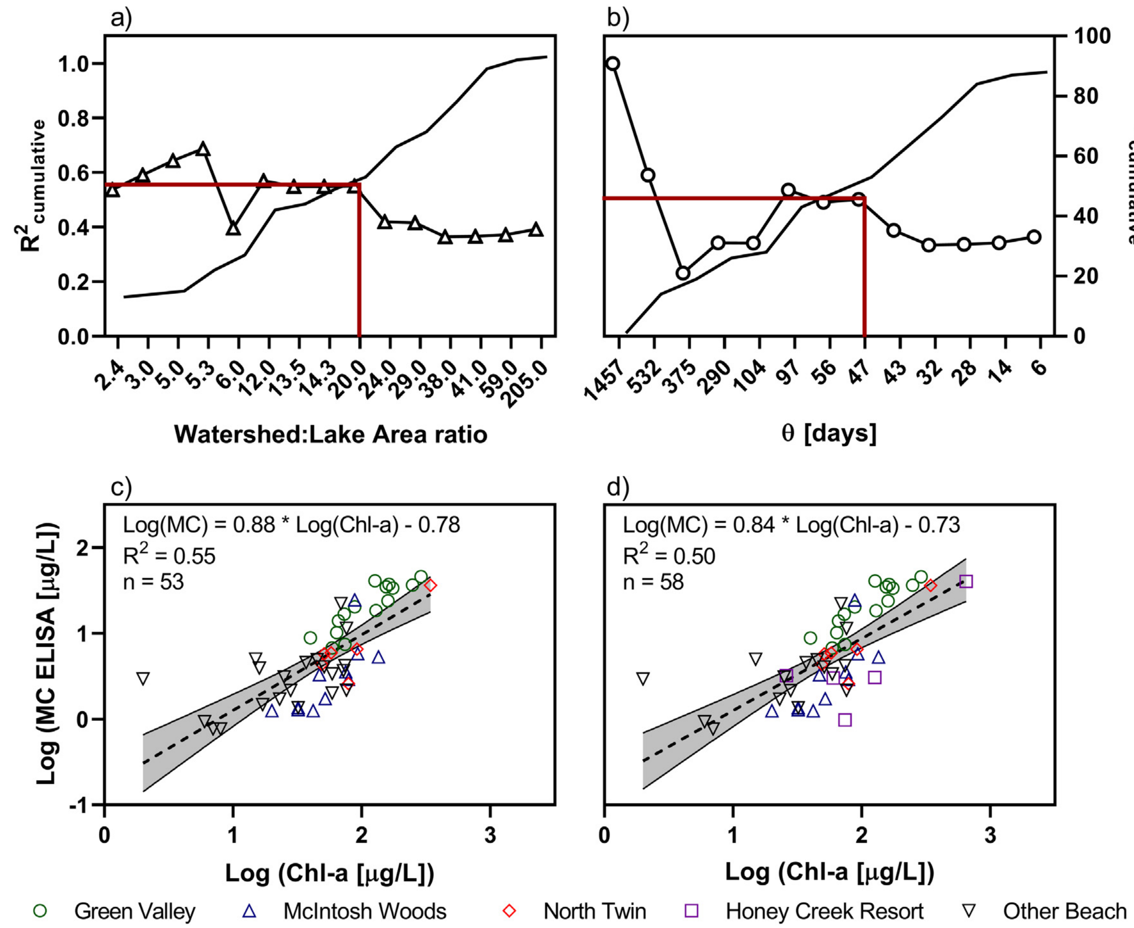

Fig. 6. Influence of lake parameters on the strength of the chlorophyll-a/microcystin relationship. Coefficient of determination (left y-axis) as a function of (a) increasing watershed:lake area, (b) decreasing residence time with corresponding sample size on right y-axis. Red lines indicate break-points for strength of chlorophyll-a/microcystin relationship for watershed: lake area ratio (20) and residence time (47 days). Linear regression of samples with (c) watershed:lake area ≤20, $p < 0.001$ and (d) residence times ≥47 days, $p < 0.001$. Increased strength of relationship for lakes with smaller watershed:lake area ($R^2 = 0.55$) and longer residence time ($R^2 = 0.50$) as compared to relationship with all lakes included ($R^2 = 0.39$).

resulted in the highest coefficient of determination at 0.18, but the slope of the regression between SHI and chlorophyll-a was not significant at the 95% confidence level ($p = 0.115$, Table 1). The next best index was BNDVI ($R^2 = 0.16$), and then SABI and NDVI ($R^2 = 0.15$). The KIVU and RedEdge algorithms performed the worst, with coefficients of determination at 0.01, and 0.02, respectively.

The SHI algorithm was developed for Lake Taihu in China and is one of the few published studies that linked the predicted chlorophyll-a values to microcystin levels (Shi et al., 2015). The relationship reported between chlorophyll-a and the index at Lake Taihu was negative, whereas our analysis yielded a positive relationship. The range of index values was greater for the Lake Taihu study, approximately −0.03 to 0.04, whereas our range of index values in the study area was approximately −0.015 to 0. In such a narrow range of index and chlorophyll-a values, it may not be possible to develop a robust linear relationship from the Green Valley case study data; this also may explain the low-degree of confidence in the slope. In fact, when applied to the Green Valley Lake data, the SHI algorithm produced unrealistic results, predicting microcystin concentrations upwards of 1000 μg/L in some areas. This is much higher than any historical data collected at the lake.

The BNDVI index was applied to Centralia Lake, Kansas in 2012 and compared to measurements of buoyant packed cell volume (Van der Merwe and Price, 2015). Buoyant packed cell volume (BPCV) is the fraction of total sample volume where buoyant cyanobacterial cells are located. Therefore, it is difficult to relate this metric to chlorophyll-a concentrations for direct comparison to the results of the Green Valley case study. Nevertheless, the range in BNDVI values were comparable (0–0.25) between one of the Kansas farm-ponds and the Green Valley case study results. BPCV explained substantially more of the variability in BNDVI values ($R^2 = 0.79$) than chlorophyll-a in our study ($R^2 = 0.16$) and thus may be a useful parameter for future investigations and monitoring.

Despite the poor relationships obtained between the algorithms and chlorophyll-a, we pursued the processing steps of converting chlorophyll-a to microcystin toxin levels to both demonstrate the potential utility of this sensing/monitoring framework and determine if emerging future improved technologies could yield a stronger remote sensing relationship. Using the summer-wide Green Valley regression developed from the state beach monitoring data (Fig. 7), we converted the BNDVI index values to predicted microcystin values, with chlorophyll-a as the intermediary. We then generated a map of predicted microcystin concentrations (Fig. 8) using the raster calculator in ArcMap.

We plotted the predicted microcystin values for each of the 15 sampling locations against measured ELISA microcystin concentrations (Fig. 8(b)) to quantify the efficacy of the BNDVI index. The predicted and measured microcystin concentrations in the Green Valley Lake study were correlated ($r = 0.43$; significant at the 89% confidence level, $p = 0.11$). Microcystin values were generally underpredicted by the BNDVI relationship by an average of 33%; however, two samples were predicted within 2% of the measured value (Site 1 and 6) and

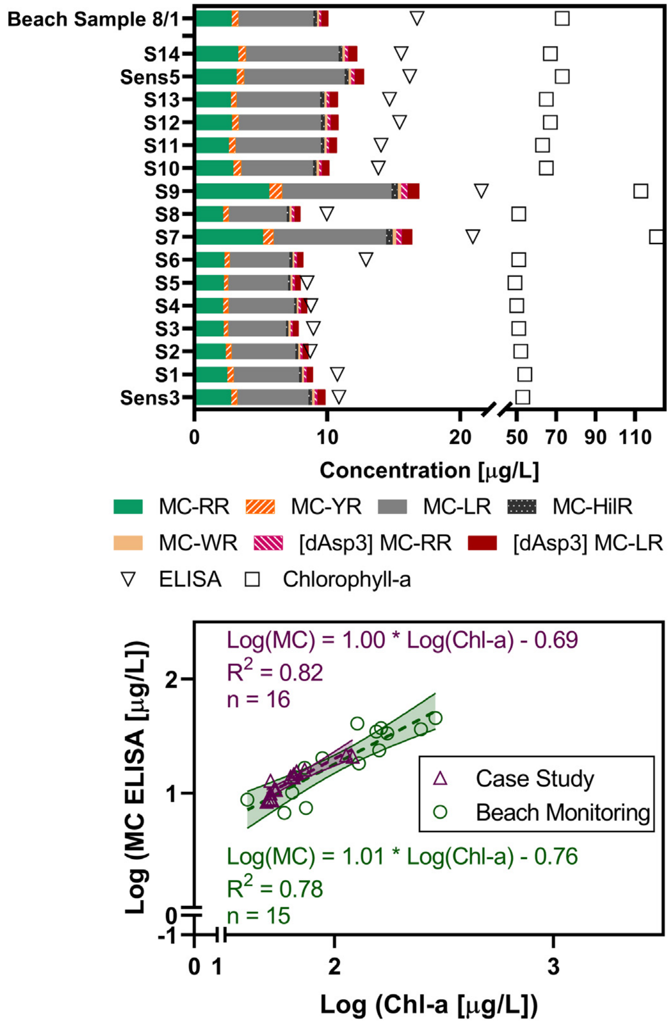

Fig. 7. (top) Distribution of microcystin congeners, chlorophyll-a, and ELISA microcystin concentrations for grab samples taken at 16 sampling sites at Green Valley Lake collected for the case study analysis on August 15, 2019. The beach monitoring data collected by the Iowa Department of Natural Resources the prior day is shown at the top for reference. (bottom) Comparison of temporally distributed state beach monitoring (green) collected throughout 2019 and spatially distributed case study (purple) chlorophyll-a/microcystin regression analysis and congener concentrations. Slopes of the regressions were not statistically significantly different ($p = 0.96$).

five samples were overpredicted by an average of 24%. Sample site 9 was the most underpredicted, 7.8 μg/L (53%) less than measured by ELISA.

From this case study, we discovered that despite the existence of a positive and significant relationship between chlorophyll-a and microcystin, remote sensing will not necessarily be an effective monitoring approach if other constraints and conditions are not met. Calibrating and testing a new model must be conducted under near ideal conditions, i.e., stable fair weather and either while the bloom has definitive spatial heterogeneity or over multiple days to adequately sample a wide range of HAB concentrations. Despite the difficulties that arose from the weather conditions of the case study, however, there is still meaningful potential for near-range remote sensing of CyanoHABs. The proposed image processing framework removes a substantial obstacle from previous over-water imaging by enabling effective image stitching. Imaging technologies are quickly advancing from the portable multispectral cameras, like the RedEdge used in this study, to lighter and more affordable hyperspectral imagers (Kislik et al., 2018). These hyperspectral cameras have narrower bands capable of more accurately predicting pigments such as chlorophyll-a or phycocyanin. The size and weight of hyperspectral cameras were previously too great for use on UAVs, but this current limitation too is changing rapidly. There is potential to develop an affordable surface water quality monitoring approach using UAVs and hyperspectral cameras to advance CyanoHAB remote sensing for small inland lakes.

For a monitoring tool to be accessible to lake managers, it would be beneficial to generate a user-interface for this new over-water image processing technique. By partnering with computer scientists/and or engineers, it would be possible to create a photogrammetry software that does not involve back-end computing by the user. Ideally, the user would be able to import images into a program such as Agisoft and would only have to select the band math algorithms to be applied and identify a few basic flight parameters. Then, the user would quickly have a toxin distribution map as output. With minimal processing time and limited custom computer code, the image processing would be accessible and useful for lake managers as a risk management tool.

4. Conclusions

We demonstrated the utility and necessity for a multi-modal monitoring approach to capture the temporal and spatial variability of CyanoHABs using a combination of analytical and remote sensing methods. The first step to generating this new framework was to better classify bloom toxicity in Iowa in the context of the status quo ELISA method. We determined that there is a critical need for the generation of more analytical congener standards and toxicological studies to fully characterize congener profiles, but the current results suggest the

Table 1
Summary of algorithm linear regressions for predicting measured chlorophyll-a concentrations applied to the data collected in the Green Valley Lake, Iowa case study.

	Band math	Linear regression equation	R^2	p-Value$_{slope}$
SHI[a]	$(e^{Red} - e^{NIR}) / (e^{Red} + e^{NIR})$	Log (Chl-a) = 13.81 ∗ SHI + 1.87	0.18	0.115
BNDVI[b]	(NIR − Blue) / (NIR + Blue)	Log (Chl-a) = −1.64 ∗ BNDVI + 2.07	0.16	0.139
SABI[c]	(NIR − Red) / (Blue + Green)	Log (Chl-a) = −1.42 ∗ SABI + 1.88	0.15	0.155
NDVI[d]	(NIR − Red) / (NIR + Red)	Log (Chl-a) = −1.81 ∗ NDVI + 1.94	0.15	0.157
FLH Blue[e]	Green − (Red + (Blue − Red))	Log (Chl-a) = −2.53 ∗ FLHBlue + 1.91	0.13	0.183
Kab1[f]	1.67–3.94 ∗ ln(Blue) + 3.78 ∗ ln(Green)	Log (Chl-a) = −0.04 ∗ Kab1 + 1.86	0.09	0.273
NDRE[g]	(NIR − RedEdge) / (NIR + RedEdge)	Log (Chl-a) = −0.67 ∗ RedEdge + 2.04	0.02	0.582
KIVU[h]	(Blue − Red) / Green	Log (Chl-a) = 0.54 ∗ KIVU + 1.85	0.01	0.702

[a] (Van der Merwe and Price, 2015).
[b] (Alawadi et al., 2010).
[c] (Mishra et al., 2009).
[d] (Beck et al., 2016).
[e] (Kabbara et al., 2008).
[f] (Barnes et al., 2000).
[g] (Brivio et al., 2001).
[h] (Shi et al., 2015).

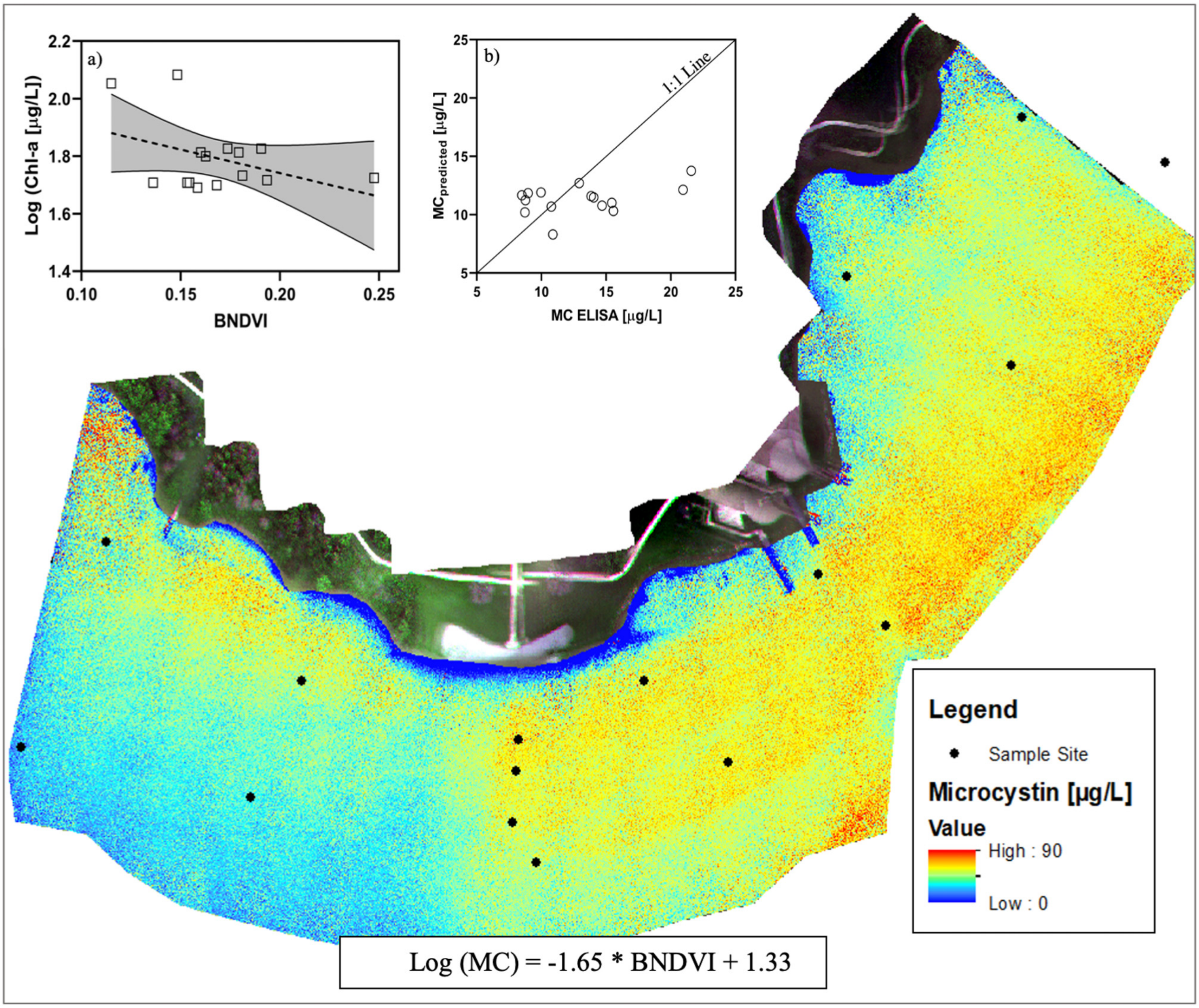

Fig. 8. Microcystin map generated from novel image processing approach, BNDVI index results, and chlorophyll-a/microcystin regression for Green Valley Lake data collected during a case study on August 15th 2019. Inset plot of linear regression between BNDVI and log of chlorophyll-a (a) and comparison of BNDVI predicted microcystin concentration and measured ELISA microcystin concentrations (b). Shaded region of inset plot (a) are 95% confidence intervals.

ELISA method may be a conservative estimate for toxicity. We demonstrated that in Iowa lakes, there is a significant and positive relationship between chlorophyll-a and ELISA microcystin concentrations that, although variable between lakes, can help predict the distribution of algal toxins. We developed and proposed a new image processing technique to overcome the current limitations of photogrammetry software, and conclude a multispectral camera is insufficient for estimating pigment concentrations under most conditions. As hyperspectral imaging becomes more affordable and laboratory measurements of phycocyanin improve, more targeted predictions of cyanobacteria will be possible. CyanoHABs have significant implications for public and ecosystem health, therefore improving our understanding and characterization is critically important. This study illuminates areas for different monitoring strategies and generates a framework for better understanding the complex spatiotemporal dynamics of HABs, as well as provides a defined foundation for areas of future research need.

CRediT authorship contribution statement

Sarah B. Douglas Greene: Conceptualization, Methodology, Software, Formal analysis, Investigation, Data curation, Writing - original draft, Visualization, Project administration. **Gregory H. LeFevre:** Conceptualization, Methodology, Resources, Writing - review & editing, Supervision, Project administration, Funding acquisition. **Corey D. Markfort:** Conceptualization, Methodology, Resources, Writing - review & editing, Supervision, Project administration, Funding acquisition.

Declaration of competing interest

The authors declare that they have no known competing financial interests or personal relationships that could have appeared to influence the work reported in this paper.

Acknowledgement

This work was supported by grants from the University of Iowa Center for Health Effects of Environmental Contamination (CHEEC) and the National Science Foundation (NRT Grant DGE 1633098). Additional funding provided by NSF Iowa EPSCoR (Award # 1101284). We would like to acknowledge partners at the State Hygienics Laboratory (Michele Yacoppuci, Melanie Kruse, Michael Schueller); the Iowa Department of

Natural Resources (Daniel Kendall); Iowa State University (Grace Wilkinson); Iowa Lakeside Laboratory (Mary Skopec, Dennis Heimdal); and the University of Iowa (Tony Loeser, Marc Linderman, Greg Ewing).

Appendix A. Supplementary data

Additional method details, statistical analysis, quality assurance/control, additional detailed data/results/analysis in figures and tables. Supplementary data to this article can be found online at https://doi.org/10.1016/j.scitotenv.2020.143327.

References

Alawadi, F., Campus, W., Dock, E., 2010. Detection of Surface Algal Blooms Using the Newly Developed Algorithm Surface Algal Bloom Index (SABI). vol. 7825, pp. 1–14. https://doi.org/10.1117/12.862096.

Altaner, S., Puddick, J., Wood, S.A., Dietrich, D.R., 2017. Adsorption of ten microcystin congeners to common laboratory-ware is solvent and surface dependent. Toxins (Basel) 9, 1–15. https://doi.org/10.3390/toxins9040129.

Arar, E.J., Collins, G.B., 1997. In Vitro Determination of Chlorophyll a and Pheophytin a in Marine and Freshwater Algae by Fluorescence. National Exposure Research Laboratory Office of Research and Development U. S. Environmental Protection Agency, pp. 1–22.

Barnes, E.M., Clarke, T.R., Richards, S.E., Colaizzi, P.D., Haberland, J., Kostrzewski, M., Waller, P., Choi, C., Riley, E., Thompson, T., Lascano, R.J., Li, H., Moran, M.S., 2000. Status and canopy density using ground-based. Fifth International Conference on Precision Agriculture (Madison, WI).

Beck, R., Zhan, S., Liu, H., Tong, S., Yang, B., Xu, M., Ye, Z., Huang, Y., Shu, S., Wu, Q., Wang, S., Berling, K., Murray, A., Emery, E., Reif, M., Harwood, J., Young, J., Nietch, C., Macke, D., Martin, M., Stillings, G., Stump, R., Su, H., 2016. Comparison of satellite reflectance algorithms for estimating chlorophyll-a in a temperate reservoir using coincident hyperspectral aircraft imagery and dense coincident surface observations. Remote Sens. Environ. 178, 15–30. https://doi.org/10.1016/j.rse.2016.03.002.

Borbor-Cordova, M.J., Torres, G., Mantilla-Saltos, G., Casierra-Tomala, A., Rafael Bermúdez, J., Renteria, W., Bayot, B., 2019. Oceanography of harmful algal blooms on the Ecuadorian coast (1997-2017): integrating remote sensing and biological data. Front. Mar. Sci. 6. https://doi.org/10.3389/fmars.2019.00013.

Bouaïcha, N., Miles, C.O., Beach, D.G., Labidi, Z., Djabri, A., Benayache, N.Y., Nguyen-quang, T., 2019. Structural diversity, characterization and toxicology of microcystins. Toxins (Basel), 11 https://doi.org/10.3390/toxins11120714.

Brivio, P.A., Giardino, C., Zilioli, E., 2001. Determination of chlorophyll concentration changes in Lake Garda using an image-based radiative transfer code for Landsat TM images. Int. J. Remote Sens. 22, 487–502. https://doi.org/10.1080/014311601450059.

Chorus, I., Bartram, J., 1999. Toxic Cyanobacteria in Water: A Guide to Their Public Health Consequences, Monitoring and Management.

Da, M., Lima, G., Teixeira, C., Da, M., Nascimento, C.O., Cia, V.L., Carvalho, P.D.E., Dos, M., Pereira, S., Hager, E., 1993. Gastroenteritis epidemic in the area of the Itaparica Dam, Bahia, Brazil1. Bull Pan Am Heal. Organ 27.

Davis, R.F., Moore, C.C., Napp, J.M., Zaneveld, J.R.V., 1997. Reducing the effects of fouling on chlorophyll estimates derived from long-term deployments of optical instruments. J. Geophys. Res. 102, 5851–5855.

Díez-quijada, L., Prieto, A.I., Guzmán-guillén, R., Jos, A., Cameán, A.M., 2019. Occurrence and toxicity of microcystin congeners other than MC-LR and MC-RR: a review. Food Chem. Toxicol. 125, 106–132. https://doi.org/10.1016/j.fct.2018.12.042.

Enzo Life Sciences Inc., n.d. Enzo life sciences product listing [WWW document]. URL https://www.enzolifesciences.com/product-listing/.

EPA, 2012. Cyanobacteria and Cyanotoxins: Information for Drinking Water Systems. United States Environ. Prot. Agency, pp. 1–9.

EPA, 2016. Water Treatment Optimization for Cyanotoxins.

EPA, 2019. Nutrient Pollution: Harmful Algal Blooms [WWW Document].

Faassen, E., Lurling, M., 2013. Occurrence of the microcystins MC-LW and MC-LF in Dutch surface waters and their contribution to total microcystin toxicity. Mar. Drugs 11, 2643–2654. https://doi.org/10.3390/md11072643.

Francy, D.S., Graham, J.L., Stelzer, E.A., Ecker, C.D., Brady, A.M., Struffolino, P., Loftin, K.A., 2015. Water quality, cyanobacteria, and environmental factors and their relations to microcystin concentrations for use in predictive models at Ohio Lake Erie and Inland Lake recreational sites, 2013–14, USGS Scientific Investigations Report 2015-5120. https://doi.org/10.3133/sir20155120.

Graham, J.L., Loftin, K.A., Meyer, M.T., Ziegler, A.C., 2010. Cyanotoxin mixtures and taste-and-odor compounds in cyanobacterial blooms from the Midwestern United States. Environ. Sci. Technol. 44, 7361–7368.

Hollister, J.W., Kreakie, B.J., 2016. Associations Between Chlorophyll a and Various Microcystin Health Advisory Concentrations [Version 2; Peer Review: 1 Approved, 2 Approved With Reservations]. pp. 1–24.

Hudnell, H.K., 2008a. Cyanobacterial Harmful Algal Blooms: State of the Science and Research Needs, Cyanobacterial Harmful Algal Blooms: State of the Science and Research Needs. https://doi.org/10.1007/978-0-387-75865-7.

Hudnell, K., 2008b. Cyanobacterial Harmful Algal Blooms: State of the Science and Research Needs. Springer Science.

IDNR, n.d. AQuIA: water quality monitoring [WWW document]. URL https://programs.iowadnr.gov/aquia/.

Ikenberry, C., 2012. Water Quality Improvement Plan for Lake Keomah.

Jones, M., Pinto, E., Torres, M., Dörr, F., Mazur-Marzec, H., Szubert, K., Tartaglione, L., Dell'Aversano, C., Miles, C., Beach, D., McCarron, P., Sivonen, K., Fewer, D., Jokela, J., Janssen, E., 2020. Comprehensive Database of Secondary Metabolites From Cyanobacteria. https://doi.org/10.1101/2020.04.16.038703.

Kabbara, N., Benkhelil, J., Awad, M., Barale, V., 2008. Monitoring water quality in the coastal area of Tripoli (Lebanon) using high-resolution satellite data monitoring water quality in the coastal area of Tripoli (Lebanon) using high-resolution satellite data. ISPRS J. Photogramm. Remote Sens. 63, 488–495. https://doi.org/10.1016/j.isprsjprs.2008.01.004.

Kasinak, J.M.E., Holt, B.M., Chislock, M.F., Wilson, A.E., 2014. Benchtop fluorometry of phycocyanin as a rapid approach for estimating cyanobacterial biovolume. J. Plankton Res. 37, 248–257. https://doi.org/10.1093/plankt/fbu096.

Kislik, C., Dronova, I., Kelly, M., 2018. UAVs in support of algal bloom research: a review of current applications and future opportunities. Drones 2, 35. https://doi.org/10.3390/drones2040035.

Micasense Inc, 2017. Image Processing.

Miller, T.R., Bartlett, S.L., Weirich, C.A., Hernandez, J., 2019. Automated subdaily sampling of cyanobacterial toxins on a buoy reveals new temporal patterns in toxin dynamics. Environ. Sci. Technol. 53, 5661–5670. https://doi.org/10.1021/acs.est.9b00257.

Mishra, S., Mishra, D.R., Schluchter, W.M., 2009. A novel algorithm for predicting phycocyanin concentrations in cyanobacteria: a proximal hyperspectral remote sensing. Remote Sens. 1, 758–775. https://doi.org/10.3390/rs1040758.

Munoz, G., Vo Duy, S., Roy-Lachapelle, A., Husk, B., Sauvé, S., 2017. Analysis of individual and total microcystins in surface water by on-line preconcentration and desalting coupled to liquid chromatography tandem mass spectrometry. J. Chromatogr. A 1516, 9–20. https://doi.org/10.1016/j.chroma.2017.07.096.

Natumi, R., Janssen, E.M.L., 2020. Cyanopeptide co-production dynamics beyond mirocystins and effects of growth stages and nutrient availability. Environ. Sci. Technol. 54, 6063–6072. https://doi.org/10.1021/acs.est.9b07334.

NOAA, 2019. Harmful algal bloom monitoring and forecasting in the Gulf of Mexico [WWW document]. URL. coastwatch.noaa.gov/cw/stories/how-our-data-are-used/harmful-algal-bloom-monitoring-and-forecasting-in-the-gulf-of-mexico.html.

Paerl, H.W., Hill, C., Hill, C., Carolina, N., Scott, J.T., 2010. Throwing fuel on the fire: synergistic effects of excessive nitrogen inputs and global warming on harmful algal blooms. Environ. Sci. Technol. Viewp. 44, 7756–7758. https://doi.org/10.1021/es102665e.

Paerl, H.W., Gardner, W.S., Havens, K.E., Joyner, A.R., Mccarthy, M.J., Newell, S.E., Qin, B., Scott, J.T., 2016. Mitigating cyanobacterial harmful algal blooms in aquatic ecosystems impacted by climate change and anthropogenic nutrients. Harmful Algae 54, 213–222. https://doi.org/10.1016/j.hal.2015.09.009.

Shi, K., Zhang, Y., Xu, H., Zhu, G., Qin, B., Huang, C., Liu, X., Zhou, Y., Lv, H., 2015. Long-term satellite observations of microcystin concentrations in Lake Taihu during cyanobacterial bloom periods. Environ. Sci. Technol. 49, 6448–6456. https://doi.org/10.1021/es505901a.

Taranu, Z.E., Pick, F.R., Creed, I.F., Zastepa, A., Watson, S.B., 2019. Meteorological and nutrient conditions influence microcystin congeners in freshwaters. Toxins (Basel) 11, 1–21. https://doi.org/10.3390/toxins11110620.

Testai, E., Buratti, F.M., Funari, E., Manganelli, M., Vichi, S., Arnich, N., Biré, R., Fessard, V., Sialehaamoa, A., 2016. Review and Analysis of Occurrence, Exposure and Toxicity of Cyanobacteria Toxins in Food.

Turner, P.C., Gammie, A.J., Codd, G.A., Hospital, G.E., Kew, J., Gross, M., Chapman, P., 1990. Pneumonia associated with contact with cyanobacteria Shy-Drager syndrome presenting as isolated paralysis of vocal cord abductors. BMJ 300, 1440–1441.

U.S. EPA, 2015. Method 545: Determination of Cylindrospermopsin and Natoxin-a in Drinking Water by Liquid Chromatography Electrospray Ionization Tandem Mass Spectrometry (LC/ESI-MS/MS).

Van der Merwe, D., Price, K.P., 2015. Harmful algal bloom characterization at ultra-high spatial and temporal resolution using small unmanned aircraft systems. Toxins (Basel) 7, 1065–1078. https://doi.org/10.3390/toxins7041065.

World Health Organization, 1998. Cyanobacterial Toxins: Microcystin-LR in Drinking-water Background Document for Development of WHO Guidelines for Drinking-water Quality.

World Health Organization, 2004. Guidelines for Drinking-water Quality, 3rd edition. https://doi.org/10.1016/S1462-0758(00)00006-6.

Zaffiro, A., Rosenblum, L., Wendelken, S., 2016. Method 546: Determination of Total Microcystins and Nodularins in Drinking Water and Ambient Water by Adda Enzyme-linked Immunosorbent Assay.